European Radiology (2019) 29:2958–2967
https://doi.org/10.1007/s00330-018-5949-2

CHEST

Integrative nomogram of CT imaging, clinical, and hematological features for survival prediction of patients with locally advanced non-small cell lung cancer

Linlin Wang[1] · Taotao Dong[2] · Bowen Xin[3] · Chongrui Xu[3] · Meiying Guo[1,4] · Huaqi Zhang[1,5] · Dagan Feng[3] · Xiuying Wang[3] · Jinming Yu[1]

Received: 16 July 2018 / Revised: 7 November 2018 / Accepted: 4 December 2018 / Published online: 14 January 2019

Abstract

Objectives To determine the integrative value of clinical, hematological, and computed tomography (CT) radiomic features in survival prediction for locally advanced non-small cell lung cancer (LA-NSCLC) patients.

Methods Radiomic features and clinical and hematological features of 118 LA-NSCLC cases were firstly extracted and analyzed in this study. Then, stable and prognostic radiomic features were automatically selected using the consensus clustering method with either Cox proportional hazard (CPH) model or random survival forest (RSF) analysis. Predictive radiomic, clinical, and hematological parameters were subsequently fitted into a final prognostic model using both the CPH model and the RSF model. A multimodality nomogram was then established from the fitting model and was cross-validated. Finally, calibration curves were generated with the predicted versus actual survival status.

Results Radiomic features selected by clustering combined with CPH were found to be more predictive, with a C-index of 0.699 in comparison to 0.648 by clustering combined with RSF. Based on multivariate CPH model, our integrative nomogram achieved a C-index of 0.792 and retained 0.743 in the cross-validation analysis, outperforming radiomic, clinical, or hematological model alone. The calibration curve showed agreement between predicted and actual values for the 1-year and 2-year survival prediction. Interestingly, the selected important radiomic features were significantly correlated with levels of platelet, platelet/lymphocyte ratio (PLR), and lymphocyte/monocyte ratio (LMR) (p values all < 0.05).

Conclusions The integrative nomogram incorporated CT radiomic, clinical, and hematological features improved survival prediction in LA-NSCLC patients, which would offer a feasible and practical reference for individualized management of these patients.

Key Points

- *An integrative nomogram incorporated CT radiomic, clinical, and hematological features was constructed and cross-validated to predict prognosis of LA-NSCLC patients.*
- *The integrative nomogram outperformed radiomic, clinical, or hematological model alone.*
- *This nomogram has value to permit non-invasive, comprehensive, and dynamical evaluation of the phenotypes of LA-NSCLC and can provide a feasible and practical reference for individualized management of LA-NSCLC patients.*

Keywords Non-small cell lung cancer · Radiomics · Nomogram · Prognosis

Linlin Wang and Taotao Dong contributed equally to this work.

✉ Xiuying Wang
xiu.wang@sydney.edu.au

✉ Jinming Yu
sdyujinming@163.com

[1] Department of Radiation Oncology, Shandong Cancer Hospital Affiliated to Shandong University, Shandong Academy of Medical Science, No. 440, Ji Yan Road, Jinan 250017, China

[2] Department of Gynecology and Obstetrics, Qilu Hospital of Shandong University, Jinan, China

[3] School of Information Technologies, the University of Sydney, Building J12, Sydney, NSW 2006, Australia

[4] Medical College of Shandong University, Jinan, China

[5] Tianjin Medical University, Tianjin, China

Abbreviations

CCRT	Concurrent chemotherapy and radiotherapy
C-index	Concordance index
CPH	Cox proportional hazard
CT	Computed tomography
GLCM	Gray-level co-occurrence matrix
GLSZM	Gray-level size zone matrix
GTV	Gross tumor volume
LA-NSCLC	Locally advanced non-small cell lung cancer
LMR	Lymphocyte/monocyte ratio
NLR	Neutrophil/lymphocyte ratio
PLR	Platelet/lymphocyte ratio
RECIST	Response Evaluation Criteria in Solid Tumors
RSF	Random survival forest

Introduction

Non-small cell lung cancer (NSCLC) accounts for 85% of lung cancer cases, with approximately one third of those being defined as locally advanced disease (LA-NSCLC), classified as stage III NSCLC [1, 2]. Although concurrent chemotherapy and radiotherapy (CCRT) is considered the standard treatment, outcomes of the LA-NSCLC patients remain poor, with a median survival of 12–23.2 months [3–5]. The TNM-based one-size-fits-all strategy might not be suitable for all patients. Identification of patients at high risk of recurrence and death would be valuable for guiding the enhanced therapy. Therefore, individualized evaluation of the prognosis for this complex and heterogenous entity is particularly important.

Computational radiomics analysis maximizes the information obtaining from the diagnostic images acquired in routine clinical practice and has proven promising results in the diagnosis, response prediction, and survival prognosis for several types of cancer patients [6–8]. In NSCLC, from computed tomography (CT) images, the quantitative measure of cancer volume reduction after chemoradiation provided more clinical information on tumor response than conventional response assessment (Response Evaluation Criteria in Solid Tumors, RECIST) [9]. In addition, 18F-fluorodeoxyglucose (FDG) positron-emission tomography (PET) features of lung cancer were found to be significantly correlated with T stages, N status, pathological stages, and tumor grades [10–13]. Several attempts have been made to improve the performance of predictive models. For instance, a grading system combined with neutrophil and SUVpeak in PET images was developed by Schernberg et al, which could effectively stratify patients with better overall survival ($hr = 5.8$, $p = 0.001$) [14]. However, these radiomic models have not taken into account the clinically indispensable clinicopathological or hematological predictors in LA-NSCLC studies, and the prognostic performance of radiomics is yet to further improve.

Emerging evidence demonstrated that hematological inflammatory cells could effectively predict the survival of patients with LA-NSCLC [15]. The mutual interaction between tumor and inflammatory cells promoted the evolution and development of cancers. On one hand, NSCLC could drive the stimulation of inflammatory cells in the tumor microenvironment as well as that in systemic circulation systems. On the other hand, these inflammatory cells could play a pivotal role in the initiation and development of NSCLC [16, 17]. Due to the important roles of systemic inflammatory cells in the biology of NSCLC, our hypothesis is that the incorporation of these inflammatory parameters with current radiomic models could improve the predictive capacity.

Nomogram, a more interpretable, graphical representation of predictive models that can include different types of predictive markers, has become the focus of interest in the cancer research in recent years [18–20]. In this study, we aim to elucidate the predictive potential of radiomic, clinicopathological, and hematological features for survival of LA-NSCLC. Further, a comprehensive nomogram integrating radiomic, clinicopathological, and hematological markers will be established.

Materials and methods

Characteristics of patients

This study retrospectively includes 118 cases of LA-NSCLC patients from Shandong Cancer Hospital between January 2014 and January 2016. The institutional review board of Shandong Cancer Hospital has approved this retrospective study of these patients. Inclusion criteria include the following: patients were aged 18 years or older, were diagnosed with stage III NSCLC confirmed by histopathology and radiographic exams according to the AJCC eighth edition TNM classification and staging system, and received CCRT without prior therapy or the operations. The exclusion criteria are patients with (1) autoimmune disease; (2) active lung infections judged by clinicians with the consideration of fever, rales, or the abnormal blood test findings of abruptly increased erythrocyte sedimentation rate (ESR), C-reactive protein (CRP), and neutrophils; (3) the pneumonitis or abscesses not related to the tumor; or (4) other infections such as gastroenteritis, appendicitis, and cholecystitis.

Clinicopathological and hematological parameters

For each patient, we collected the clinicopathological characteristics including age at diagnosis, gender, tumor location, tumor size, node metastasis status, histological types, Karnofsky performance scores (KPS), radiation types and doses, concurrent chemotherapy types, usage of consolidative

chemotherapy, and pre- and post-therapeutical serum tumor biomarkers including CEA, NSE, and Cyfra 211. KPS is to quantify patient's ability to tolerate therapy in terms of their physical function and ability to take care of themselves and to perform daily activity.

Hematological inflammatory variables included levels of monocytes, neutrophils, lymphocytes, hemoglobin, and platelet counts. Also, neutrophil/lymphocyte ratio (NLR), lymphocyte/monocyte ratio (LMR), and platelet/lymphocyte ratio (PLR) were calculated for each patient. For each patient, both the pre- and post-therapeutical hematological variables ("1" and "2" were used as markers, respectively) were obtained.

Follow-up and prognostic evaluations

Follow-up data were collected from the most recent medical records of these patients, including the information of physical exams, complete blood count, blood biochemistry, tumor biomarkers, thoracic CT scans, and abdominal ultrasound. In addition, we also acquired the survival information of these patients through telephone enquiries, medical insurance records, and death certificates. Overall survival in this study was defined as the period from the date of admission to the death date regardless of specific causes of death.

Image segmentation and radiomic feature extraction

For each patient in this study, we have collected both pre- and post-CCRT contrast-enhanced CT images using a SOMATOM Definition AS (Siemens Healthineers). The CT parameters were as follows: tube voltage, 120 kVp; tube current, 200 mAs; detector, 64 × 0.625 mm; beam pitch, 1.5. The overall workflow of this study is illustrated in Fig. 1. First of all, 3D gross tumor volume (GTV) was interactively segmented and delineated using an in-house segmentation software based on random walker algorithm [21, 22]. This delineation procedure was performed twice on all the CT images with the interval about 2 months between the first and second evaluations to reduce the operator's biases.

In total, 1045 comprehensive CT image features, including intensity, shape, texture, and wavelets [6] were extracted from 118 LA-NSCLC cases. Intensity features were calculated by the first-order statistics through the tumor voxel intensity distributions. Shape features were extracted to reflect 3D geometric features of the tumor, such as surface area, compactness, and tumor volume. Texture features were described using texture matrix such as gray-level co-occurrence matrix (GLCM) and gray-level size zone matrix (GLSZM) to quantify internal tumor heterogeneity and using log filters to depict different tumor coarseness with different sigma values [23]. Wavelet features could extract intensity and texture features in the frequency domain using wavelet decomposition on the original images.

Statistical analyses

Important feature selection Stable radiomic features were selected from the two delineations using the Pearson correlation analyses. Consensus clustering method combining with Cox proportional hazard (CPH) was then used for the selection of prognostic features based on the p value ranking. Clustering combined with random survival forest (RSF), an ensemble tree method for analyzing right-censored survival data, was used to generate trees and was performed for comparison. Clinicopathological and hematological parameters with prognostic value were also selected using multivariate CPH regression model.

Prognostic model establishment Multimodal features and parameters including radiomic, clinicopathological, and inflammatory features were fused into a single predictive model based on multivariate CPH model. Performance of this model was evaluated with the concordance index (C-index). For comparison, in the RSF model, the possible split points for each variable were examined to find the optimal split method.

Cross-validation Bootstrap based cross-validation was applied to assess and compare the discriminative power of CPH model and RSF model. These prediction models were trained on 10% of total bootstrap samples drawn with replacement from the original data while tested in the observations that were not in the training sets. Then, the C-index was computed for different time points (with a constant interval of 1 month), and the means of those C-indexes were calculated to represent the model discriminative ability [24].

Nomogram construction Model with better C-index was chosen for further nomogram construction. Calibration curves of nomogram were then drawn for 1-year and 2-year overall survival of the patients. The calibration curves illustrated both survival probabilities predicted by nomogram and the observed probabilities.

All statistical analyses are two-sided, with the significance level of 0.05. Statistical analyses were performed with "rms," "Hmisc," "survival," "pec," and "randomForestSRC" modules in R programming language and environment (http://www.r-project.or) as well as in STATA software (version 14.1).

Results

Clinical parameters of the patients

For all of the 118 LA-NSCLC cases, 48 patients were TNM stage IIIA (40.7%), 58 cases were stage IIIB (49.2%), and 12 patients were stage IIIC (10.2%). The median survival of these

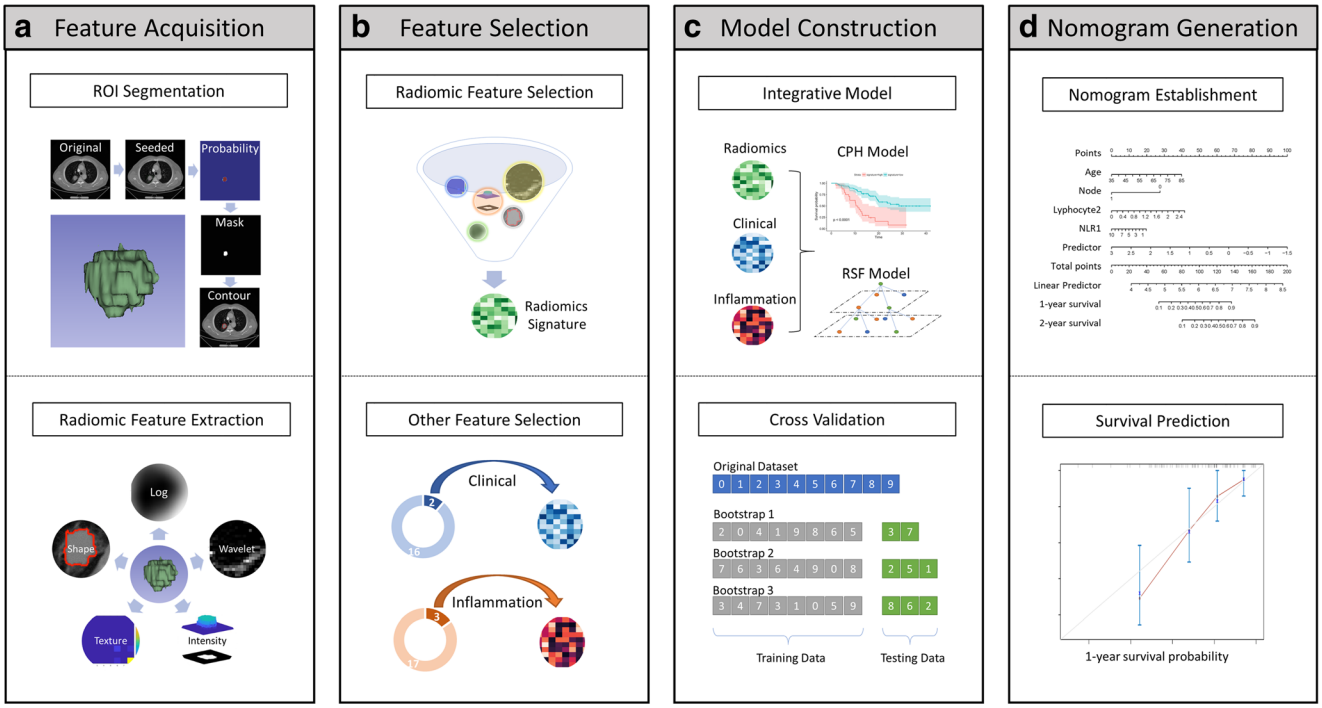

Fig. 1 Workflow of generation of a comprehensive radiomic-based nomogram. **a** Examples of CT images were obtained from included LA-NSCLC patients and were delineated (upper panel); features are extracted from the defined tumor regions of CT images, including intensity, shape, texture, log, and wavelet texture (lower panel). **b** Predictive radiomic, clinicopathological, and hematological features are selected. **c** Prognostic features are fitted into one predictive model using CPH and RSF models, respectively (upper panel). Cross-validations are performed for these two models, and it was found that CPH is more reliable in our study (lower panel). **d** Nomogram for 1-year and 2-year overall survival is generated for these patients (upper panel). Calibration curves are drawn for the nomogram-predicted and actual survival of patients (lower panel). LA-NSCLC, locally advanced non-small cell lung cancer; CPH, Cox progression hazards; ROI, region of interest; RSF, random survival forest

patients is 19.8 months (95% confidence interval 4.0–35.6 months). Other clinicopathological characteristics were shown in Table 1.

Important radiomic feature selection

In total, 1045 radiomic features were extracted from the CT images including 70 sets of pre-CCRT and 97 sets of post-CCRT. We first ranked the stability of the 1045 features using Pearson's correlation coefficients calculated between the two delineations. As a result, 829 stable features were selected for the subsequent analyses (Fig. 2a). Then, two hybrid selection methods, i.e., clustering combined with CPH and clustering combined with RSF, were used and compared in our study. Features selected by clustering combined with CPH were found to be more predictive with a C-index of 0.699 in comparison to 0.648. Radiomic features extracted from post-treatment CT images were found to be superior in prediction than that from pre-treatment CT images (Fig. 2b). Thus, features from post-treatment CT images were selected by the method of clustering combined with CPH and were further investigated in the following study (Fig. 2b).

With backward elimination algorithm, the least prognostic features were repeatedly removed from the clustered feature subset until the subset was able to achieve the optimal predictive performance. Then, the top eight prognostic features selected from the clusters were analyzed with further correlation analyses to avoid overfitting (Fig. 2c). After identifying pairs of highly correlated features (Pearson's correlation coefficient > 0.9), the one with higher p value in each pair was eliminated. Finally, four independent predictive radiomic features, i.e., wavelet-LHL_glcm_JointAverage, wavelet-LLL_glcm_ClusterProminence, original_glcm_ClusterShade, and log-sigma-5-0-mm-3D_firstorder_Maximum, were used to generate the radiomic signature which also had a good predictive capacity in the Kaplan-Meier analyses of these patients (Fig. 2d).

Association of selected features with hematological inflammatory variables

Due to the importance of the inflammatory factors in the prognosis prediction of patients with NSCLC, we further explored the correlation of selected features with the hematological inflammatory variables. Two of the four selected features were found to be significantly correlated with specific inflammatory factors. In particular, the "wavelet_LHL_glcm_JointAverage" feature was positively correlated with levels of platelet1 and PLR1 while negatively correlated with levels of LMR2 significantly ($p = 0.026$, $p = 0.045$, and $p = 0.048$, respectively). In addition, the "log_sigma_5_0_mm_3D_firstorder_Maximum"

Table 1 Patient characteristics

Characteristic	All patients ($N = 118$)	
	N	%
Age (years)		
≥ 60	62	52.5
> 60	56	47.5
Gender		
Male	104	88.1
Female	14	11.9
KPS		
≥ 80	112	94.9
< 80	6	5.1
Location		
Central	82	69.5
Peripheral	36	30.5
Histology subtype		
SCC	66	55.9
Non-SCC	52	44.1
T stage		
T1	8	6.8
T2	37	31.3
T3	21	17.8
T4	52	44.1
N stage		
N0	12	10.1
N1	14	11.9
N2	57	48.3
N3	35	29.7
Radiotherapy technique		
3D-CRT	50	42.4
IMRT	68	57.6
Radiotherapy doze (Gy)		
≤ 60	96	81.4
> 60	22	18.6
Concurrent chemotherapy		
EP	13	11
PC	39	33.1
Others	66	55.9

feature was significantly positively correlated with both pre- and post-therapeutic platelet levels ($p = 0.013$ and $p = 0.049$, respectively) (Fig. 3).

Performance of multimodality prediction model

Patient age and lymph node metastases were found to be independent risk factors in our study using multivariate CPH. In addition, for the inflammatory parameters, lymphocyte2 levels and NLR1 were found to be independent prognostic factors for our patient cases.

Next, multivariate CPH and RSF were used and compared for assessing the performance of the predictive model. C-index of CPH and RSF was not stable until 505 days, and C-index thereafter was selected for our study. The C-index of the CPH model was 0.792 and it retained 0.743 after cross-validation (Fig. 4a, b). In comparison, C-index of the RSF model dropped from 0.891 to 0.647 when cross-validation was performed (Fig. 4a, b). Again, the CPH model was found to be more stable and was ascertained for the further construction of nomogram.

Importantly, the performance of this integrative model was proven to be superior to radiomic, clinicopathological, or hematological model alone, with C-indexes of 0.699, 0.618, and 0.653, respectively.

Performance interpretation with nomogram

Nomogram for prediction performance (Fig. 5a) of 1-year and 2-year survival was generated on the basis of the selected radiomic signature, patient age, lymph node metastasis, lymphocyte2 levels, and NLR1.

Further, a calibration curve had been drawn for these patients. The estimated versus observed 1-year and 2-year survival probabilities intersected the 45° line, showing that the predicted value approximated the observed value within a 95% confidence interval (Fig. 5b, c). This calibration curve had shown agreement between predicted and actual values.

Discussion

In this study, we incorporated comprehensive multimodal radiomic, clinicopathological, and hematological factors for the individualized survival prediction of LA-NSCLC patients. To the best of our knowledge, for the first time, a concise nomogram with only five variables can provide a feasible and practical reference to clinical professionals for recommending a more appropriate management for LA-NSCLC patients. We also found that the selected radiomic features were associated with inflammatory variables in these patients, suggesting that systemic inflammatory status may partially account for the poor survival of patients harboring these radiomic features.

The performance of the integrative model was also shown to be superior to the individual model alone in our present study, demonstrating powerful predicting capability using different types of biomarkers. As reported, the C-index of the radiomic model was often between 0.60 and 0.67, which has been improved to 0.72 when combining with clinical and genomic features [25–28]. This improvement due to information integration of the distinct sources may reflect that multiple

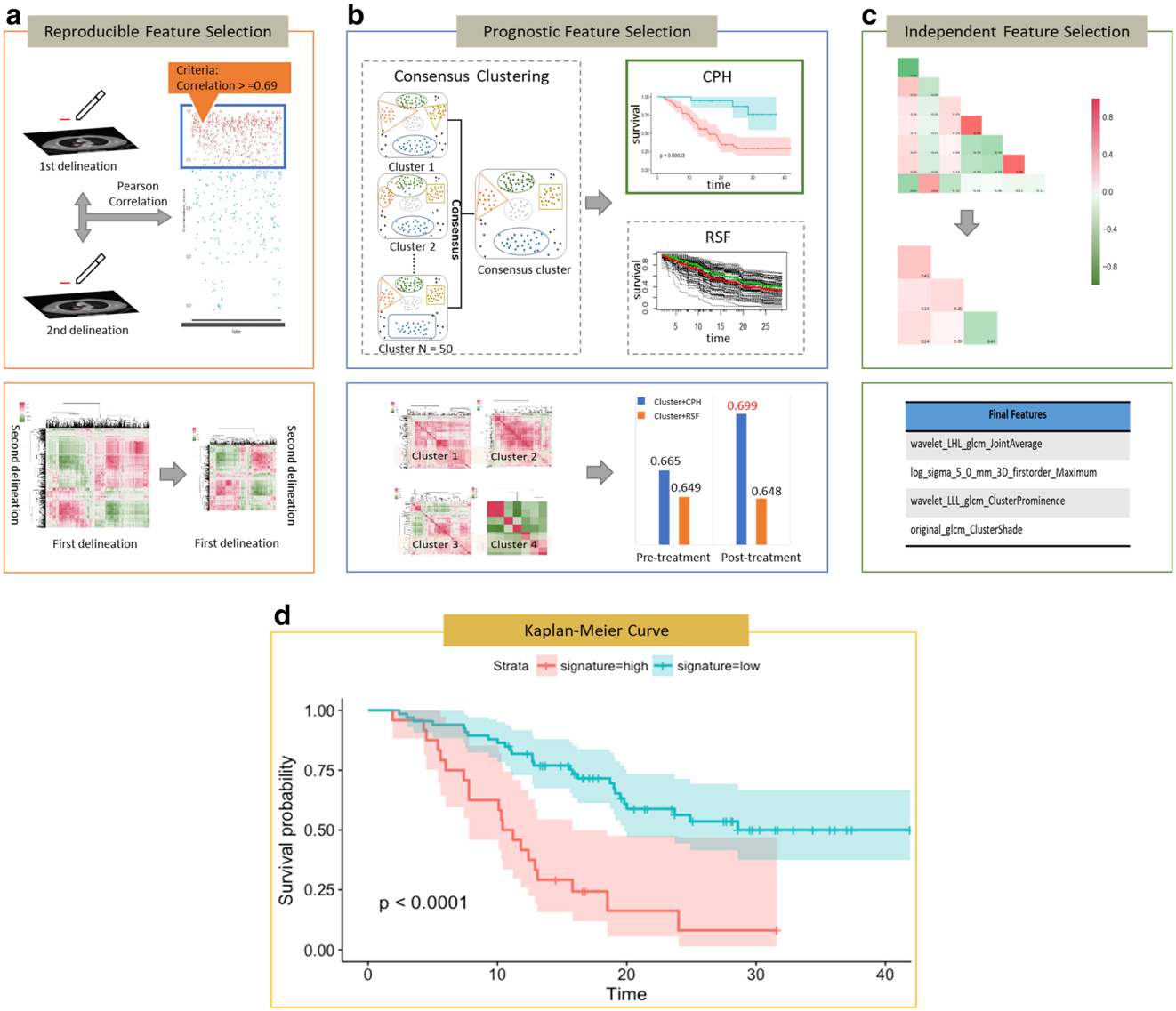

Fig. 2 Radiomic feature selection. **a** Correlation analyses are performed for the features extracted from two delineations. **b** All features are divided into four clusters by clustering method. Features selected by CPH are more predictive than those selected by RSF. Also, features from post-treatment are better than those from pre-treatment (lower panel). **c** Further correlation analyses are performed for the prognostic features to select the independent predictive features. Finally, four features are selected for the radiomic signature. **d** Predictive capacity of radiomic signature. Kaplan-Meier curve shows that this radiomic signature could effectively discriminate patients with better survival from those with worse survival

factors of the patient characteristics contributing to a more accurate prediction model. In comparison to using genomic features, our new nomogram incorporating the clinical, hematological, and CT imaging data, which are all routinely evaluated in the clinical settings, could be more feasible in clinical practice.

Most studies correlating radiomics with survival outcomes in lung cancers analyzed the baseline features of pre-treatment [29, 30]. However, tumors undergo dynamic changes during treatment, which would be more informative [31–33]. Thus, we further analyzed the CT features pre- and post-CCRT dynamically. Rather than keeping the same set of important radiomic features from baseline for analyzing post-treatment CT data [26], we selected the important prognostic features of pre- and post-treatment, respectively. Our analysis on these features found that the performance of the post-treatment features was much higher than that of the baseline features, which demonstrated that post-treatment features were able to better reflect the actual response to CCRT and were more informative and accurate for predicting the patients' prognosis. This finding suggests that CT scan after CCRT is also recommended for LA-NSCLC patients.

Interestingly, our selected radiomic features were found to be associated with inflammatory biomarkers including levels

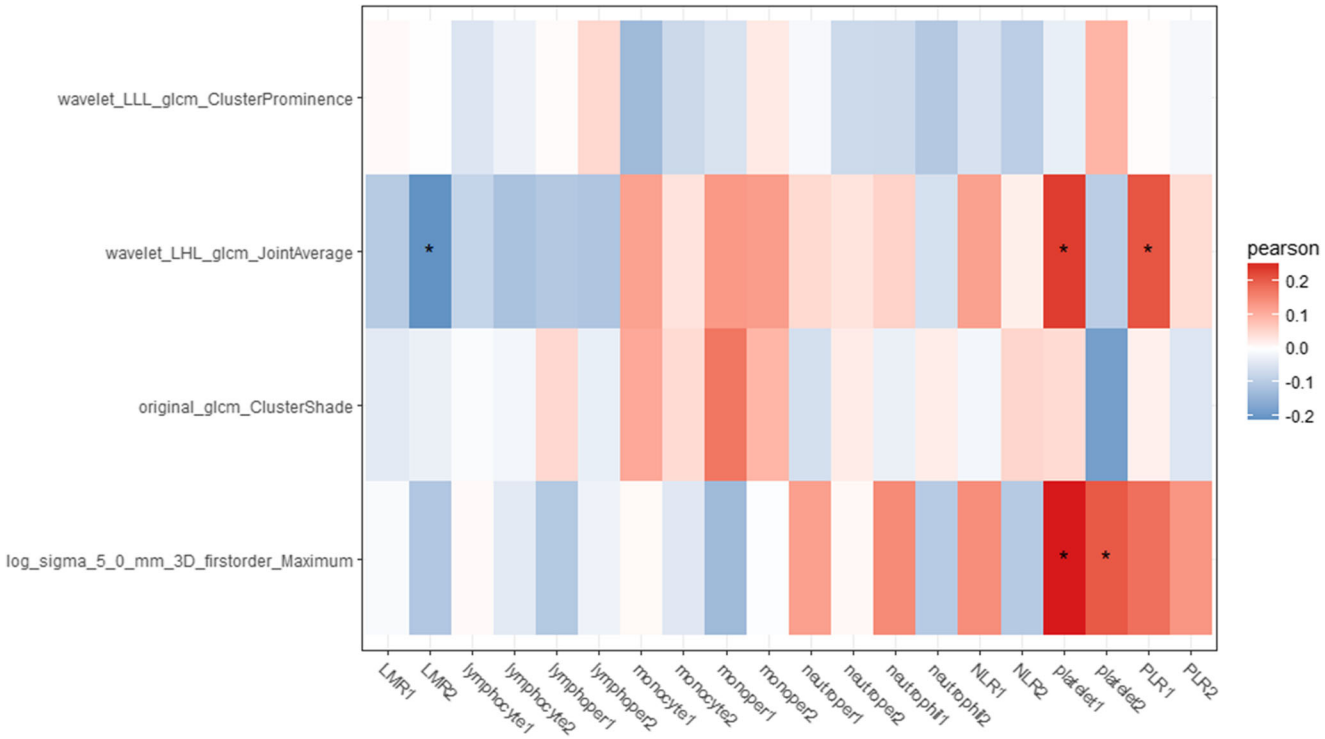

Fig. 3 Correlation analyses of selected radiomic features with hematological inflammatory cells. Selected radiomic features are also analyzed for the correlation with inflammatory cells for included patients. Red bars show the positive correlation while the blue ones denote the negative association. Bars with asterisk denote the correlation has reached significance. LMR, lymphocyte/monocyte ratio; NLR, neutrophil/lymphocyte ratio; PLR, platelet/lymphocyte ratio; 1, pre-treatment data; 2, post-treatment data

of platelet, LMR, and PLR. Platelets play a role in protecting tumor cells from antitumor immunity and releasing cytokines for tumor progression [34]; monocytes have been proven as an important factor in favoring tumor invasion and metastasis by producing protease enzymes [35, 36]. In contrast, lymphocytes are a protective factor by inducing cytotoxic cell death and inhibiting tumor cell proliferation and migration [37]. Hence, the elevated platelet or PLR and the decreased LMR are considered to be associated with worse prognosis of patients due to their important roles in the initiation and development of cancers [38–40]. Our study found that radiomic feature "wavelet_LHL_glcm_JointAverage" or "log_sigma_5_0_mm_3D_firstorder_Maximum" positively correlated with levels of platelet1 or PLR1 while negatively correlated with LMR2. These radiomic features may indicate the unfavorable immunological status which at least partly accounts for the prognostic effects of radiomic features in LA-NSCLC patients. Yet, the mechanism underlying the predictive capacities of the radiomic features and their relationship with inflammatory biomarkers still need to be further investigated.

We investigated both the effects of CPH and that of RSF for feature selection and model fitting and found that CPH was much more stable and reliable than RSF. Although RSF could

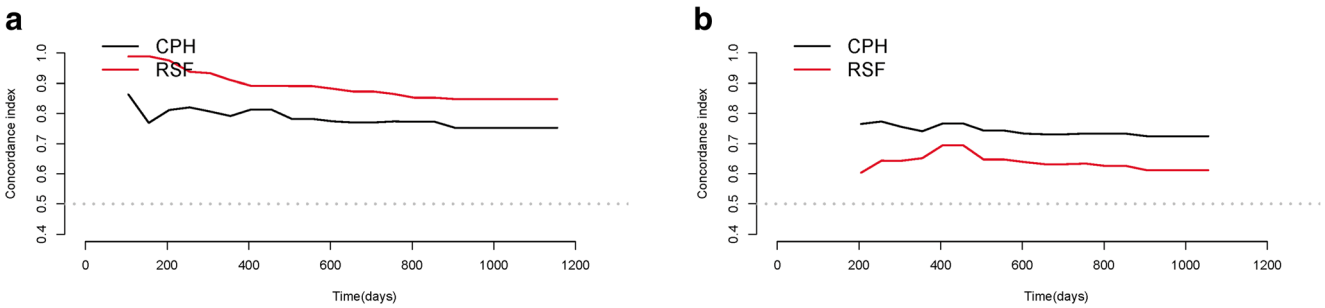

Fig. 4 Predictive models are established with different methods. **a** C-indexes of the model including radiomic, clinicopathological, and inflammatory parameters using CPH and RSF methods are shown. **b** Cross-validations are performed for these two kinds of methods. CPH model is shown to be more reliable than RSF model in our study

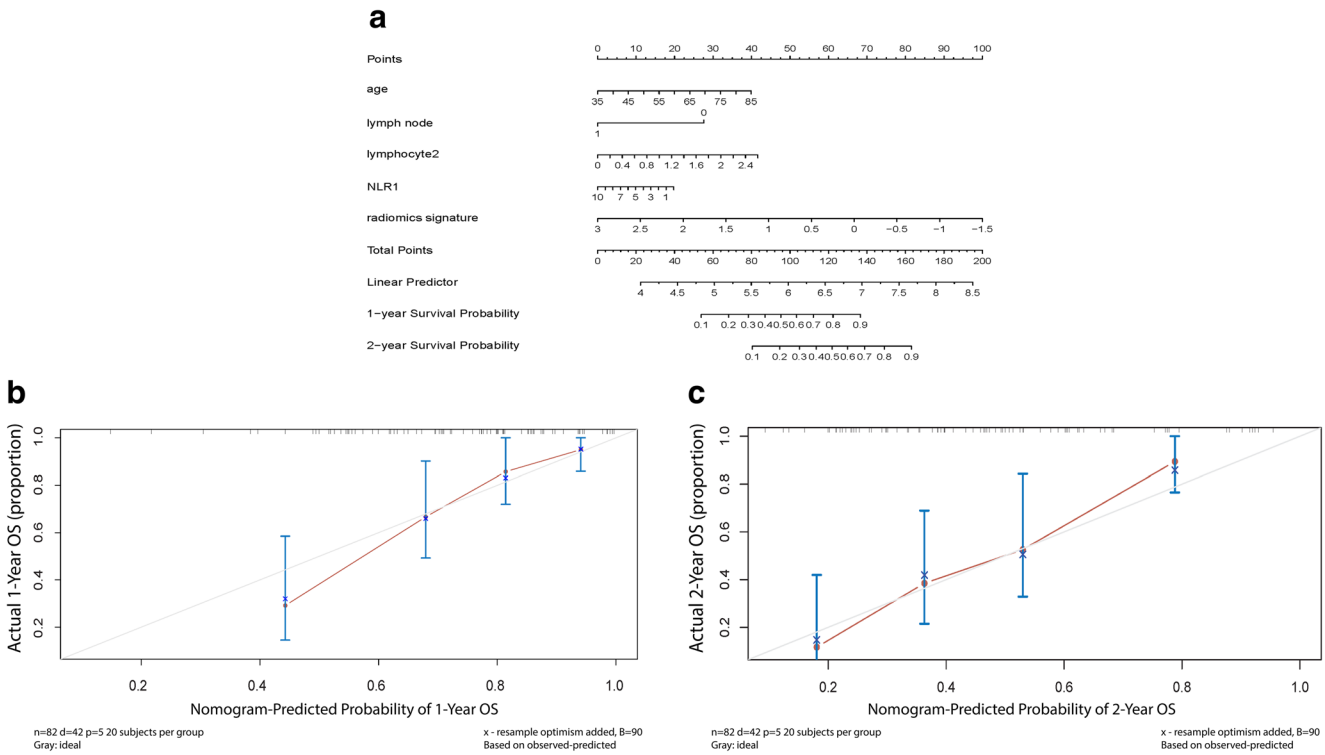

Fig. 5 Generation and evaluation of nomogram. **a** A comprehensive nomogram for prediction of 1-year and 2-year overall survival for patients with LA-NSCLC. **b** Calibration curve for estimation of 1-year overall survival predicted by nomogram. Nomogram-estimated overall survival is plotted on the (*x*)-axis; actual overall survival is plotted on the *y*-axis. Dash line represents the ideal agreement. **c** Calibration curve of 2-year overall survival predicted by nomogram for patients with LA-NSCLC

reach higher C-index in the primary model establishment analysis, the C-index dropped remarkably in the subsequent cross-validation stages, which was consistent with the reported findings in glioblastoma research [23, 41]. We speculate that selection of algorithm in the machine learning model establishment stage would be influenced by the sample size of the study. Only when the sample size is sufficiently large could we include a bigger amount of parameters in machine learning models while avoid the risk of overfitting.

There are some limitations in our present study. Firstly, due to 32 patients were not confirmed the cause of death, we therefore only analyzed OS for evaluating the patient prognosis. In the future study, it could be better if cancer-specific survival is investigated for the prediction of patients with LA-NSCLC. Secondly, this was a retrospective study, and prospective trials in different centers and regions could eliminate the selection bias. In addition, the underlying mechanism for explaining the prognostic role of our nomogram still needs to be further investigated in the future. The analysis of genomic types with different driving genes might be helpful for understanding the biological characteristics of the patients with poor outcomes who harbor the worse integrative features of radiomics, clinicopathologics, and hematology simultaneously.

In conclusion, we have constructed a simple, yet not trivial, nomogram integrating radiomic, clinicopathological, and hematological parameters, which would have potential as an individualized utility in the clinical practice for LA-NSCLC patients. This nomogram has value to permit non-invasive, comprehensive, and dynamical evaluation of the phenotypes of LA-NSCLC and to predict the survival prognostication for LA-NSCLC patients.

Funding This work was supported by China Scholarship Fund, the Project of Postdoctoral Science Foundation of China (Grant Nos. 2016M590640 and 2016M592199), the Project of Postdoctoral Innovation of Shandong Province (Grant No. 201501010), National Health and Family Planning Commission of China (201402011), and National Natural Science Foundation of China (81472812).

Compliance with ethical standards

Guarantor The scientific guarantor of this publication is Jinming Yu.

Conflict of interest The authors of this manuscript declare no relationships with any companies whose products or services may be related to the subject matter of the article.

Statistics and biometry No complex statistical methods were necessary for this paper.

Informed consent Written informed consent was waived by the Institutional Review Board.

Ethical approval Institutional Review Board approval was obtained.

Methodology
• prospective
• diagnostic or prognostic study
• performed at one institution

References

1. Jemal A, Bray F, Center MM, Ferlay J, Ward E, Forman D (2011) Global Cancer Statistics. CA Cancer J Clin 61:69–90
2. Yang P, Allen MS, Aubry MC et al (2005) Clinical features of 5,628 primary lung cancer patients: experience at Mayo Clinic from 1997 to 2003. Chest 128:452–462
3. Aupérin A, Le Péchoux C, Rolland E et al (2010) Meta-analysis of concomitant versus sequential radiochemotherapy in locally advanced non-small-cell lung cancer. J Clin Oncol 28:2181–2190
4. Hanna N, Neubauer M, Yiannoutsos C et al (2008) Phase III study of cisplatin, etoposide, and concurrent chest radiation with or without consolidation docetaxel in patients with inoperable stage III non–small-cell lung cancer: the Hoosier Oncology Group and U.S. Oncology. J Clin Oncol 26:5755–5760
5. Vokes EE, Herndon JE 2nd, Kelley MJ et al (2007) Induction chemotherapy followed by chemoradiotherapy compared with chemoradiotherapy alone for regionally advanced unresectable stage III non–small-cell lung cancer: cancer and leukemia group B. J Clin Oncol 25:1698
6. Aerts HJ, Velazquez ER, Leijenaar RT et al (2014) Decoding tumour phenotype by noninvasive imaging using a quantitative radiomics approach. Nat Commun 5:4006
7. Gillies RJ, Kinahan PE, Hricak H (2016) Radiomics: images are more than pictures, they are data. Radiology 278:563–577
8. Lambin P, Leijenaar RTH, Deist TM et al (2017) Radiomics: the bridge between medical imaging and personalized medicine. Nat Rev Clin Oncol 14:749
9. Agrawal V, Coroller TP, Ying H et al (2016) Radiologic-pathologic correlation of response to chemoradiation in resectable locally advanced NSCLC. Lung Cancer 102:1
10. Hatt M, Majdoub M, Vallières M et al (2015) 18F-FDG PET uptake characterization through texture analysis: investigating the complementary nature of heterogeneity and functional tumor volume in a multi-cancer site patient cohort. J Nucl Med 56:38–44
11. Kirienko M, Gallivanone F, Sollini M et al (2017) FDG PET/CT as theranostic imaging in diagnosis of non-small cell lung cancer. Front Biosci (Landmark Ed) 22:1713
12. Desseroit MC, Visvikis D, Tixier F et al (2016) Erratum to: development of a nomogram combining clinical staging with 18F-FDG PET/CT image features in non-small-cell lung cancer stage I–III. Eur J Nucl Med Mol Imaging 43:1477–1485
13. Pyka T, Bundschuh RA, Andratschke N et al (2015) Textural features in pre-treatment [F18]-FDG-PET/CT are correlated with risk of local recurrence and disease-specific survival in early stage NSCLC patients receiving primary stereotactic radiation therapy. Radiat Oncol 10:100
14. Schernberg A, Reuze S, Orlhac F et al (2018) A score combining baseline neutrophilia and primary tumor SUV_{peak} measured from FDG PET is associated with outcome in locally advanced cervical cancer. Eur J Nucl Med Mol Imaging 45:187–195
15. Scilla KA, Bentzen SM, Lam VK et al (2017) Neutrophil-lymphocyte ratio is a prognostic marker in patients with locally advanced (stage IIIA and IIIB) non-small cell lung cancer treated with combined modality therapy. Oncologist 22:737–742
16. Bremnes RM, Al-Shibli K, Donnem T et al (2011) The role of tumor-infiltrating immune cells and chronic inflammation at the tumor site on cancer development, progression, and prognosis: emphasis on non-small cell lung cancer. J Thorac Oncol 6:824–833
17. Schreiber RD, Old LJ, Smyth MJ (2011) Cancer immunoediting: integrating immunity's roles in cancer suppression and promotion. Science 331:1565–1570
18. Oberije C, De Ruysscher D, Houben R et al (2015) A validated prediction model for overall survival from stage III non-small cell lung cancer: toward survival prediction for individual patients. Int J Radiat Oncol Biol Phys 92:935
19. Tanadini-Lang S, Rieber J, Filippi AR et al (2017) Nomogram based overall survival prediction in stereotactic body radiotherapy for oligo-metastatic lung disease. Radiother Oncol 123:182–188
20. Tang XR, Li YQ, Liang SB et al (2018) Development and validation of a gene expression-based signature to predict distant metastasis in locoregionally advanced nasopharyngeal carcinoma: a retrospective, multicentre, cohort study. Lancet Oncol 19:382–393
21. Cui H, Wang X, Zhou J et al (2015) Topology polymorphism graph for lung tumor segmentation in PET-CT images. Phys Med Biol 60:4893–4914
22. Cui H, Wang X, Zhou J et al (2018) A topo-graph model for indistinct target boundary definition from anatomical images. Comput Methods Programs Biomed 159:211–222
23. Leger S, Zwanenburg A, Pilz K et al (2017) A comparative study of machine learning methods for time-to-event survival data for radiomics risk modelling. Sci Rep 7:13206
24. Gerds TA, Kattan MW, Schumacher M, Yu C (2013) Estimating a time-dependent concordance index for survival prediction models with covariate dependent censoring. Stat Med 32:2173–2184
25. Grossmann P, Stringfield O, El-Hachem N et al (2017) Defining the biological basis of radiomic phenotypes in lung cancer. Elife 6:e23421
26. Fave X, Zhang L, Yang J et al (2017) Delta-radiomics features for the prediction of patient outcomes in non–small cell lung cancer. Sci Rep 7:588
27. Lee J, Li B, Cui Y et al (2018) A quantitative CT imaging signature predicts survival and complements established prognosticators in stage I non-small cell lung cancer. Int J Radiat Oncol Biol Phys 102:1098–1106
28. Huang Y, Liu Z, He L et al (2016) Radiomics signature: a potential biomarker for the prediction of disease-free survival in early-stage (I or II) non-small cell lung cancer. Radiology 281:947
29. Ohri N, Duan F, Snyder BS et al (2016) Pretreatment 18FDG-PET textural features in locally advanced non-small cell lung cancer: secondary analysis of ACRIN 6668/RTOG 0235. J Nucl Med 57:228–233
30. Salavati A, Duan F, Snyder BS et al (2017) Optimal FDG PET/CT volumetric parameters for risk stratification in patients with locally advanced non-small cell lung cancer: results from the ACRIN 6668/RTOG 0235 trial. Eur J Nucl Med Mol Imaging 44:1969–1983
31. Rao SX, Lambregts DM, Schnerr RS et al (2016) CT texture analysis in colorectal liver metastases: a better way than size and volume measurements to assess response to chemotherapy? United European Gastroenterol J 4:257–263
32. Dong X, Sun X, Sun L et al (2016) Early change in metabolic tumor heterogeneity during chemoradiotherapy and its prognostic value for patients with locally advanced non-small cell lung cancer. PLoS One 11:e0157836
33. Cunliffe A, Armato SG 3rd, Castillo R, Pham N, Guerrero T, Al-Hallaq HA (2015) Lung texture in serial thoracic computed tomography scans: correlation of radiomics-based features with radiation therapy dose and radiation pneumonitis development. Int J Radiat Oncol Biol Phys 91:1048–1056

34. Cox G, Walker RA, Andi A, Steward WP, O'Byrne KJ (2000) Prognostic significance of platelet and microvessel counts in operable non-small cell lung cancer. Lung Cancer 29:169–177
35. Balkwill F, Mantovani A (2001) Inflammation and cancer: back to Virchow? Lancet 357:539–545
36. Galdiero MR, Garlanda C, Jaillon S, Marone G, Mantovani A (2013) Tumor associated macrophages and neutrophils in tumor progression. J Cell Physiol 228:1404–1412
37. Smith HA, Kang Y (2013) The metastasis-promoting roles of tumor-associated immune cells. J Mol Med (Berl) 91:411–429
38. Liu HB, Gu XL, Ma XQ et al (2013) Preoperative platelet count in predicting lymph node metastasis and prognosis in patients with non-small cell lung cancer. Neoplasma 60:203–208
39. Li Y, Jia H, Yu W et al (2016) Nomograms for predicting prognostic value of inflammatory biomarkers in colorectal cancer patients after radical resection. Int J Cancer 139:220–231
40. Cannon NA, Meyer J, Iyengar P et al (2015) Neutrophil–lymphocyte and platelet–lymphocyte ratios as prognostic factors after stereotactic radiation therapy for early-stage non–small-cell lung cancer. J Thorac Oncol 10:280–285
41. Gittleman H, Lim D, Kattan MW et al (2017) An independently validated nomogram for individualized estimation of survival among patients with newly diagnosed glioblastoma: NRG Oncology RTOG 0525 and 0825. Neuro Oncol 19:669–677